Contemporaneous and recent radiations of the world's major succulent plant lineages

Mónica Arakaki[a], Pascal-Antoine Christin[a], Reto Nyffeler[b], Anita Lendel[b], Urs Eggli[c], R. Matthew Ogburn[a], Elizabeth Spriggs[a], Michael J. Moore[d], and Erika J. Edwards[a,1]

[a]Department of Ecology and Evolutionary Biology, Brown University, Providence, RI 02912; [b]Institut für Systematische Botanik, Universität Zürich, CH-8008 Zürich, Switzerland; [c]Sukkulenten-Sammlung Zürich, Mythenquai 88, CH-8002 Zürich, Switzerland; and [d]Department of Biology, Oberlin College, Oberlin, OH 44074

Edited* by Peter Crane, Yale School of Forestry and Environmental Studies, New Haven, CT, and approved April 12, 2011 (received for review January 13, 2011)

The cacti are one of the most celebrated radiations of succulent plants. There has been much speculation about their age, but progress in dating cactus origins has been hindered by the lack of fossil data for cacti or their close relatives. Using a hybrid phylogenomic approach, we estimated that the cactus lineage diverged from its closest relatives ≈35 million years ago (Ma). However, major diversification events in cacti were more recent, with most species-rich clades originating in the late Miocene, ≈10–5 Ma. Diversification rates of several cactus lineages rival other estimates of extremely rapid speciation in plants. Major cactus radiations were contemporaneous with those of South African ice plants and North American agaves, revealing a simultaneous diversification of several of the world's major succulent plant lineages across multiple continents. This short geological time period also harbored the majority of origins of C_4 photosynthesis and the global rise of C_4 grasslands. A global expansion of arid environments during this time could have provided new ecological opportunity for both succulent and C_4 plant syndromes. Alternatively, recent work has identified a substantial decline in atmospheric CO_2 ≈15–8 Ma, which would have strongly favored C_4 evolution and expansion of C_4-dominated grasslands. Lowered atmospheric CO_2 would also substantially exacerbate plant water stress in marginally arid environments, providing preadapted succulent plants with a sharp advantage in a broader set of ecological conditions and promoting their rapid diversification across the landscape.

climate change | paleobotany | CAM photosynthesis

Plants are generally classified as succulent when they exhibit pronounced water storage in one or more organs. High degrees of succulence are most often associated with a suite of other characteristics that together confer survival in water-limited environments. This "succulent syndrome" usually includes a shallow root system that permits rapid uptake of unpredictable precipitation; a thick, waxy cuticle that prevents excessive water loss; and Crassulacean acid metabolism (CAM), an alternative photosynthetic pathway that allows plants to uptake atmospheric CO_2 at night when water loss is minimized (1). Although some 30 plant lineages have been classified as succulent, only a small subset of those are species-rich and ecologically important elements of arid and semiarid ecosystems worldwide. These lineages include the ice plants (Aizoaceae, ≈2,000 spp), the spurges (*Euphorbia*, ≈2,100 spp., ≈650 of which are succulent), the stonecrops (Crassulaceae, ≈1,400 spp.), the aloes (*Aloe*, ≈400 spp.), the agaves (*Agave*, ≈200 spp.), the stapeliads and asclepiads (Apocynaceae-Asclepiadoideae, ≈3,700 spp., ≈1,150 of which are succulent) and especially the cacti (Cactaceae, ≈1,850 spp.) (2).

The cacti represent the most spectacular New World radiation of succulent plants. Most cacti exhibit a highly specialized life form, with extremely succulent, photosynthetic stems and leaves that have been modified into spines (3). The lineage has a broad distribution, but is most prominent in semiarid and arid regions, with several main centers of diversity in arid Mexico and the southwestern United States, the central Andes of Peru and Bolivia, and eastern Brazil (2). Despite their ecological importance, the timing of cactus origins and diversification has remained enigmatic. Previous work has emphasized the fact that the cacti are extremely diverse yet almost exclusively New World in distribution, suggesting a possible origin between 90 and 65 Ma, which would allow maximal time for diversification and a spatial separation of Africa and South America (3, 4). Others have suggested a more recent origin, because of limited molecular sequence divergence among the major cactus lineages (5, 6).

There are no relevant fossil records for cacti or their closest relatives, which has made it difficult to estimate divergence times in the group (e.g., ref. 7). However, researchers have recently made significant progress in dating the origins of major angiosperm lineages (8), and we exploited these advances to infer the timing of cactus origin and diversification with a two-step approach. First, we sequenced whole chloroplast genomes from 12 cacti and relatives (Table S1) and combined these data with a larger whole-chloroplast data matrix of 90 seed plants (8) to build a broadly sampled phylogeny of angiosperms. We then used multiple fossil calibration points within a Bayesian framework to estimate divergence times and confidence intervals for several key nodes in cacti and relatives (Fig. S1). To look more specifically at patterns and timing of diversification within the major cactus lineages, we performed a series of additional dating analyses on a second phylogeny generated from fewer loci but that included a greatly expanded taxon sampling within the cacti (Fig. 1, Fig. S2, and Table S2). We then identified the timing of major radiations in cacti and their relatives by implementing a likelihood approach that optimizes the number and placement of shifts in diversification rate across a phylogeny (9).

Results

Our analysis of 102 chloroplast genomes produced a topology and set of age estimates for major angiosperm nodes that are highly congruent with those of previous studies (8, 10) (Fig. S1). Age estimates for particular nodes were extremely robust to removing various combinations of fossil constraints (Table S3). Our phylogenomic analyses suggest that the cacti are ≈35 million years old (Ma), which is much younger than many previous assumptions (3, 4) but consistent with speculation based on limited divergence of molecular sequences (5, 6).

Author contributions: M.A. and E.J.E. designed research; M.A., P.-A.C., R.N., A.L., U.E., R.M.O., E.S., and M.J.M. performed research; M.A., P.-A.C., and E.J.E. analyzed data; and M.A. and E.J.E. wrote the paper.

The authors declare no conflict of interest.

*This Direct Submission article had a prearranged editor.

Data deposition: The sequences reported in this paper have been deposited in the GenBank database (accession nos. HQ620718–HQ621695).

[1]To whom correspondence should be addressed. E-mail: erika_edwards@brown.edu.

This article contains supporting information online at www.pnas.org/lookup/suppl/doi:10.1073/pnas.1100628108/-/DCSupplemental.

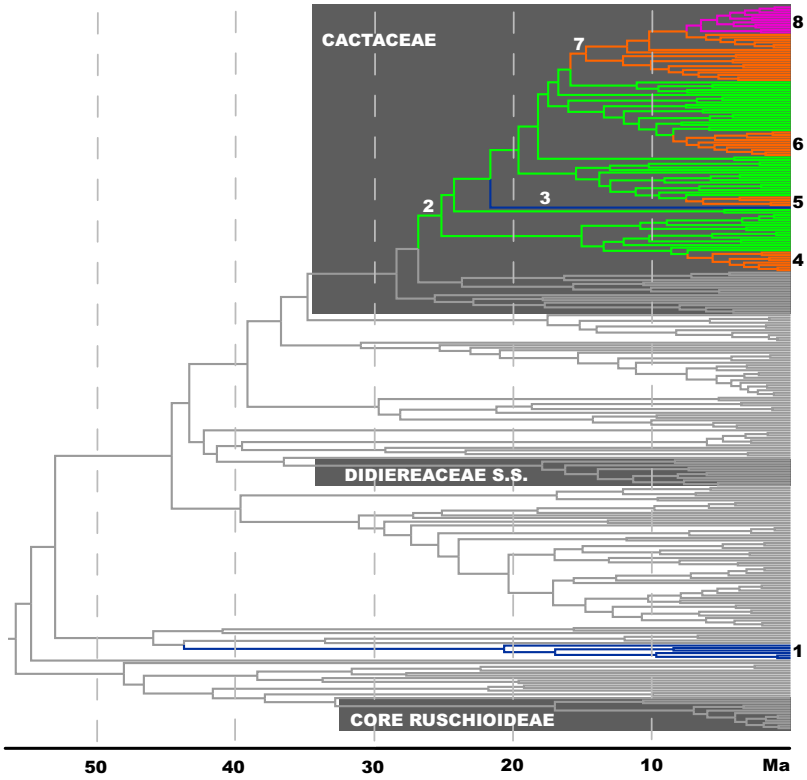

Fig. 1. Time-calibrated phylogeny of the cacti and their relatives. Colored branches indicate shifts in diversification: Blue branches represent lineages with significantly lower net diversification than the background rate; green, orange, and pink branches indicate higher diversification and/or species turnover (see Table 1 for parameter estimates and clade names). Gray boxes indicate ecologically important succulent clades: Cactaceae (New World); Malagasy Didiereaceae (Madagascar); core Ruschiodeae (Aizoaceae, Southern Africa).

Furthermore, divergence time estimates from our densely sampled phylogeny of cacti and close relatives indicates that many of the important species radiations within this group are actually quite recent (Fig. 1, Table 1, and Table S4). The paraphyletic *Pereskia* comprises the first two diverging, species-poor cactus lineages and are woody trees and shrubs with slightly succulent leaves. The succulent cactus "life-form" emerged in a step-like fashion during early cactus evolution, and certain elements, such as moderate tissue water storage, conservative water use, and variants of CAM photosynthesis, are found in *Pereskia* and other members of the Portulacineae (11, 12). Pronounced morphological succulence, as exhibited by the core cacti (13), did not evolve until ≈25 Ma and was associated with a significant increase in diversification rate (Fig. 1, number 2, and Table 1). However, the most dramatic species radiations in the cacti occurred many millions of years after the evolution of a fully succulent syndrome and were not associated with any obvious anatomical or physiological innovations. We identified five additional shifts in diversification rate in the cacti, the majority occurring within the last 8 Ma (Table 1). With the exception of the genus *Opuntia* (the prickly pears), these shifts occurred at nodes nested within or just outside named taxonomic groups (2). Our results suggest that the cactus floras of the three main centers of cactus diversity and endemism (Mexico, central Andes, and Brazil) are extremely young, and more or less contemporary. For example, the North American barrel and columnar cacti both experienced upward shifts in speciation rate

Table 1. Significant shifts in diversification rate and species turnover in cacti and relatives

Node number (see Fig. 1)	Clade	Age, Ma	*D*, lineage/Ma	*r*, lineage/Ma	ε	Center of diversity
Background rate	Portulacineae + Molluginaceae	55–53	0.137	0.095	1.0×10^{-7}	Worldwide
1	Molluginaceae pro parte	44–21	0.088	0.016	0.980	Southern Africa
2	Core cacti	27–25	0.268	0.232	0.306	Widespread in North and South America
3	*Blossfeldia liliputana*	21–0	0	2.27×10^{-17}	3.90×10^{-6}	South America
4	*Opuntia*	7.5–0	0.70	0.434	0.874	North America
5	*Mammillaria* + *Coryphantha*	7.6–6.3	0.719	0.225	0.973	Mexico
6	Hylocereinae + Echinocereinae	8.5–7.5	0.576	0.422	0.724	Mexico and Central America
7	Notocacteae + Cereeae	16.0–14.8	0.386	0.239	0.850	South America
8	Trichocereinae + Cereinae	7.5–6.5	0.768	0.432	0.903	South America

D is diversification rate under a pure-birth model ($D = [\ln(N_t) - \ln(N_o)]/T$, where T is the stem age of the clade, N_t is the number of taxa, and $N_o = 1$) (71). *r* is diversification rate ($\lambda - \mu$) and ε is a calculation of species turnover rate (μ/λ) where λ = speciation rate and μ = extinction rate, as estimated by MEDUSA (9).

roughly 8–6 Ma, which coincides with a similar shift in a clade comprising the Trichocereinae, a South American lineage that comprises the majority of cactus diversity in the central Andean region, and the Cereinae, a nearly exclusively Brazilian lineage (7.5–6.5 Ma; Table 1).

Other noteworthy succulent lineages in our analyses, although located in very different geographical regions, are also of similar age. The endemic Didiereaceae of Madagascar (Didiereaceae *s.s.*) are often called the "Cacti of the Old World," and are stem-succulent trees and shrubs of the spiny-thicket forests. While not being especially species rich (≈12 spp), their diversification began ≈17 Ma; crown *Alluaudia*, the largest and arguably most succulent lineage, is ≈11 Ma. Our crown age estimate of core Ruschioideae (the ice plants, Aizoaceae), an extremely species-rich and fundamental component of the Succulent Karoo flora of South Africa, is ≈17 Ma (Figs. 1 and 2 and Fig. S3). This node age is substantially older than a previous report that suggested a rapid radiation in this group 8.7–3.8 Ma (14); however, our taxon sampling of core Ruschioideae was too sparse to allow for investigation of diversification shifts within this group that, of course, may have occurred more recently.

Discussion

Our analyses provide strong evidence that although the cactus lineage is of moderate age, most of the extant diversity in this group was generated by significant radiations occurring throughout the mid to late Miocene and into the Pliocene. The timing of these major diversification events within cacti is extraordinarily similar to those inferred for other more distantly related succulent plant groups. Agaves, with their center of diversity in North American deserts, are reported to have had two primary pulses of rapid diversification, the first at 8–6 Ma and a second at 3–2.5 Ma (15). In South Africa, the ice plants (particularly the core Ruschioideae) comprise the fundamental element of the succulent Karoo region, and their major radiation was estimated as occurring roughly 8.7–3.8 Ma (14). Remarkably, new research in *Euphorbia* has identified many multiple independent radiations of succulent lineages, occurring across regions of Africa, Madagascar, and South America, and all within a timeframe of ≈11–2 Ma (16). While we currently lack data on the aloes, stonecrops, and asclepiads, every arid-adapted succulent lineage investigated thus far has followed a similar tempo of evolution: Although the origins of a pronounced succulent syndrome in these groups vary widely between ≈40 and 10 Ma, they all share a single timeframe of extensive global diversification in the late Miocene-Pliocene. Studies of other desert (nonsucculent) plants from various regions have also demonstrated a similar pattern of recent radiation (17–20). The simultaneous diversification of arid-adapted lineages provides a general insight into the history of the world's arid regions, which has been limited by a bias against fossil formation in dry environments. As a unique paleoclimate proxy, this timeframe is in good agreement with other evidence that the late Miocene-Pliocene witnessed the establishment of many extant desert ecosystems.

Most of the succulent radiations reported here could be reasonably linked to the expansion of aridity due to particular geological events. In North American cacti and agaves for example, radiations coincided with the establishment of the Sonoran desert, which was presumably caused by increased volcanic activity and the formation of the Gulf of California (21). This timeframe was also a period of significant Andean uplift activity, which both intensified and expanded arid environments throughout most of western South America (22). Eastern Africa was similarly experiencing increasing aridity possibly due to shifts in ocean (23) or atmospheric (24) circulation, and around this time a winter rainfall precipitation regime became established in the South African Karoo region (14, 20).

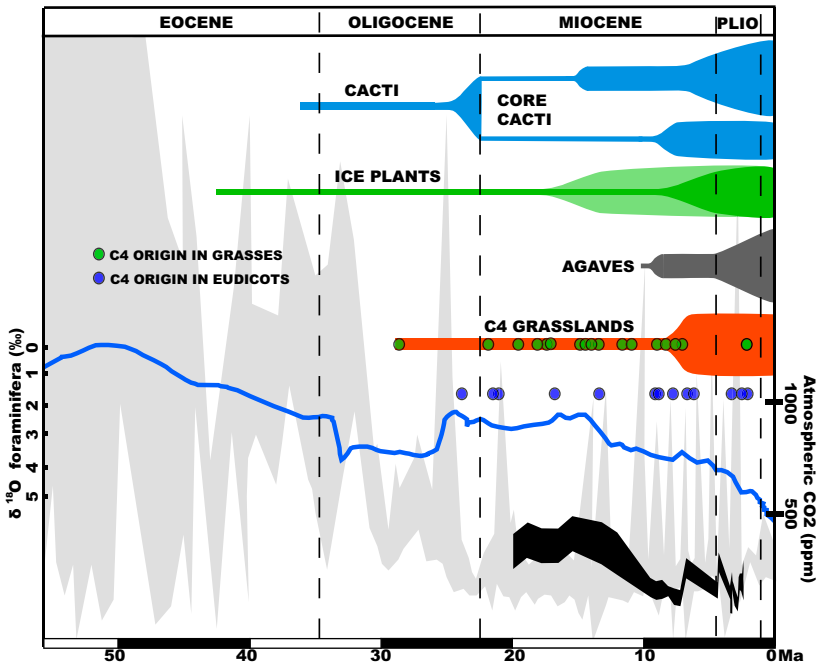

Fig. 2. CO_2, global temperature, C_4 origins, C_4 grasslands, and the diversification of succulent plants during the late Miocene/Pliocene. Lines extend back to the origin of the various succulent clades, and significant diversification events are represented by increases in line width. For the ice plants, dark green indicates timing of diversification by Klak et al. (14), and light green represents our estimated age of the same node ("core Rushioideae"; ref. 14). Blue line reflects decline in relative global temperatures, inferred from deep sea ^{18}O, which is primarily a metric of deep sea temperature and sea-ice volume. Gray area in background represents reconstructed atmospheric CO_2 levels and their uncertainty through time, collated from multiple proxies (27). Black line is the drop in CO_2 hypothesized by Tripati et al. (33).

However, the temporal concordance of these diversification events with major vegetation changes in other geographical regions suggests that a more global environmental driver may also be contributing to the expansion of drought-adapted plant communities (Fig. 2). The late Miocene has long been recognized as a fundamental moment in Earth history due to the global emergence of grasslands dominated by grasses with C_4 photosynthesis (25). C_4 photosynthesis is a highly convergent and complex trait that reduces rates of photorespiration. It is advantageous under low atmospheric CO_2 conditions and is frequently associated with plants adapted to environments that promote high levels of photorespiration, such as hot temperatures, aridity, and high salinity (26). Although the earliest known origin of C_4 photosynthesis was ≈30 Ma and coincided with an abrupt CO_2 decline in the Oligocene, most origins appeared much later (27). In fact, a global burst of evolution of the C_4 photosynthetic pathway in angiosperms, inferred both in grasses (27) and in eudicots (28), occurred during the late Miocene-Pliocene (Fig. 2). This very small window of time thus witnessed extraordinary changes in ecosystem properties worldwide: The emergence of C_4 grasslands, which cover 20–30% of the terrestrial land surface; the origins of many C_4 plant lineages, which are signature elements of most stress-adapted floras; and a pulse of rapid diversification in every major succulent plant lineage that has thus far been examined. We highlight mid-late Miocene trends in two potential environmental variables that could have provided strong ecological advantages to both succulent and C_4 syndromes.

First, a steep and steady decline in global temperatures after the mid-Miocene climate optimum is well documented from oxygen isotope records of deep-sea foraminifera (29), although the causes of this decline are still debated (30). While the relationship between temperature and precipitation is complex, drops in global temperatures may reduce global precipitation due to a slowdown of the hydrological cycle, and evidence from both paleoecological reconstructions (reviewed in ref. 27) and stable isotopes (e.g., refs. 31 and 32) from multiple continents consistently indicate a general trend toward increasing aridity during this time. Thus, irrespective of any one particular geological event, the late Miocene-Pliocene succulent and C_4 plant revolution corresponded with what appears to be a near-global phenomenon of reduced precipitation.

Second, we argue that the coincidental nature of this global succulent diversification with the rise of C_4 photosynthesis warrants another look at atmospheric CO_2 levels during the late Miocene. There has been much disagreement about CO_2 concentrations during this time; although the abrupt Oligocene decline in atmospheric CO_2 is not debated, different CO_2 proxies have produced conflicting signals regarding subsequent fluctuation (27). Most recently, Tripati et al. (33) estimated a precipitous decline in CO_2 between 15 and 8 Ma, from roughly 425 ppm to 200 ppm (Fig. 2), with further fluctuations between 200 and 300 ppm occurring into the Pleistocene. A drop of that magnitude would carry disastrous consequences for C_3 plants (26) and would have provided a strong and obvious competitive advantage to the C_4 syndrome. These same trends could also promote diversification of lineages that already possess a suite of drought-adapted traits. Declining CO_2 decreases a typical plant's water use efficiency, because the diffusion gradient between atmospheric and internal leaf CO_2 levels will be smaller and plants will need to adopt a higher stomatal conductance (and thus greater water loss) to maintain a given rate of carbon fixation. A drop in CO_2 concentration would therefore immediately expand the ecological space in which drought-adapted succulent plants, with their high photosynthetic water use efficiency, would be competitive (34).

We suggest that a rapid expansion of available habitat (rather than any particular new "key innovation") during the late Miocene was a primary driver of the global diversification of plant lineages already possessing a preadapted succulent syndrome. Against a backdrop of increasing global aridity, a sharp CO_2 decline is a plausible driver of the simultaneous expansion of C_4 grasslands, the clustering of new C_4 origins, and the diversification of succulent lineages. The contemporaneous spread of multiple C_4 and succulent plant lineages across the global landscape is a remarkable demonstration of convergence in plants, and their limited and predictable evolutionary responses to environmental stress.

Materials and Methods

Sequence Provenance and Taxon Sampling. A dataset with sequences for 79 protein-coding genes and four ribosomal RNA genes for 90 species of seed plants was obtained from Moore et al. (8). Twelve chloroplast genomes were added to increase sampling in the Caryophyllales (Table S1). Fresh young leaves or photosynthetic stems were obtained from specimens maintained in cultivation at the Brown University Plant Environmental Center or the Sukkulenten-Sammlung Zürich.

To build a phylogeny with better representation of Portulacineae and Cactaceae, plant specimens were obtained from a variety of sources (Table S2). A total of 295 taxa were included. We generated new sequences for 94 taxa for *PHYC* and 63 taxa for *matK*/*trnK* and combined these with an additional 215 *trnK*/*matK* plus 22 *PHYC* sequences from the National Center for Biotechnology Information (NCBI). Voucher specimens are deposited at the Brown University Stephen T. Olney Herbarium, the Sukkulenten-Sammlung Herbarium, Zürich; the IADIZA-CRICYT Ruiz Leal Herbarium, Mendoza, or San Marcos University Herbarium, Lima.

Chloroplast Isolation and Sequencing. Chloroplast isolations were performed by using the sucrose gradient centrifugation protocol by Jansen et al. (35) with a modification for working with succulent plant material. Samples were ground with liquid nitrogen until a coarse powder was obtained, which was quickly transferred to cold Sandbrink isolation buffer. Chloroplast lyses and whole genome amplification were performed with a Qiagen REPLI-g Midi Kit (Qiagen). Library construction and sequencing were performed at the Environmental Genomics Core Facility (EnGenCore) of the University of South Carolina, Columbia. Samples were multiplexed and prepared by following instructions for the 454 GS-FLX instrument (Roche Life Sciences). Raw data (in FASTA format), Newbler preliminary assemblies (from the Newbler software designed for the GS 20 system), quality scores, and NewblerMetrics were received from EnGenCore in standard flowgram format (sff). Alignments and partial assemblies were performed by using MIRA V3rc4 (36) and Geneious 4.8 (Biomatters). Large contigs or nearly complete assemblies were imported into DOGMA (37) for annotation, which enabled extraction of individual gene sequences.

DNA Isolation, PCR-Based Amplification, and Sequencing. Total genomic DNA was isolated from fresh or silica gel-dried tissue, using the MP FastDNA SPIN Kit and FastPrep Instrument (MP Biomedicals).

We selected the nuclear phytochrome C (*PHYC*) gene occurring as single copy and shown to be a good source of phylogenetic information (13). We also incorporated the trnK-maturase K (*trnK*/*matK*) region, which is the cp region best represented in NCBI and has also proven to be very useful for phylogenetic inference in Cactaceae and other Portulacineae [e.g., Cactaceae (6), Montiaceae (38)]. The first exon of *PHYC* (≈1.2 Kb) was amplified by using primers developed by Mathews et al. (39). The PCR protocol for *PHYC* required a high-quality Taq polymerase (Amplitaq DNA polymerase; Life Technologies) and consisted of a stepdown protocol (with a preheating step of 5 min at 94 °C) beginning at an annealing T of 65 °C and ending at 53 °C, with 2 min annealing, 1 min denaturation at 94 °C, and 1 min primer extension at 72 °C for a total of 36 cycles. Products were cloned by using the StrataClone PCR cloning kit (Agilent Technologies) and sequenced by using the M13 F/R primer pair. Sequencing was performed at the Genomics and Sequencing Center of the University of Rhode Island, using the Applied Biosystem BigDye Terminator v3.1 chemistry. Samples were run on an ABI 3130xl genetic analyzer. Primers and protocol used to amplify and sequence the *trnK*/*matK* region were developed by Christin et al. (40).

Phylogenetic Analyses. The chloroplast dataset of 12 Caryophyllales (Table S1) was added to the broader angiosperm dataset by Moore et al. (8). Nucleotide sequences of protein-coding genes were translated into amino acids, aligned automatically with MUSCLE (41), and adjusted manually with MacClade 4.05 (http://macclade.org). Each gene was aligned separately and later concatenated. Small regions that were difficult to align were excluded from the analysis. The final dataset consisted of 102 taxa, 83 genes, and 75,643 nucleotides. Sequences of *trnK*/*matK* and *PHYC* were processed as above.

Maximum likelihood (ML) analyses of the whole chloroplast matrix and *PHYC*, *trnK/matK*, and combined *PHYC-trnK/matK* datasets were performed with RAxML 7.0.4 (42) and run on the Brown University IBM iDataPlex Linux cluster.

Estimation of Divergence Times and Shifts in Diversification. Divergence times were estimated using a two-step approach recommended by Rutschmann (43), which applies a Bayesian method that accounts for variable substitution rates between lineages and over time. To start, model parameters were calculated for each of the 83 genes using baseml (PAML package; ref. 44). Branch lengths and the variance-covariance matrix were then approximated by estbranches (45). Finally a Bayesian MCMC procedure implemented in multidivtime (multidistribute package; refs. 45 and 46) was used to estimate posterior distributions of substitution rates and divergence times. The MCMC sampling procedure was run for 1 million generations, after a burn-in of 100,000 generations, with a sampling frequency of 100 generations. We ran two analyses by using 13 fossils as minimum-age node constraints: One analysis used the youngest (lower) bound of the time period to which the fossils were assigned and the second with the oldest (upper) bound. In both cases, constraints were considered minimum ages. We did a sensitivity test (using the youngest assigned ages) that included 13 alternative analyses in which one fossil constraint was excluded at a time. Additional analyses including all fossil constraints but varying MCMC parameters provided similarly consistent results.

Fossils used as calibration points are mostly mesofossils placed with high confidence in their respective phylogenetic position and time frame (Table S3) (47–62). The fossil record for Caryophyllales is scarce. We considered two candidates: *Coahuilacarpon,* consisting of infructescences of a possible Phytolaccaceae ascribed to the Campanian (63), and Amaranthaceae (*Chenopodipollis*) pollen from the early Tertiary (Paleocene) of Texas (58). We chose the latter as it is considered to be quite reliably identified (S. Manchester and D. M. Jarzen, personal communication). A well described fossil from the Eocene of Australia has been confidently placed within Caryophyllaceae (59); however, our taxon sampling did not allow us to make good use of this fossil, because it could only be placed at the same node as *Chenopodipollis*, which is older. Poaceae fossils (e.g., refs. 64 and 65) are more difficult to place because of insufficient taxon sampling in the present analysis. We assigned a minimum age of 34 Ma to the crown group of Poaceae based on data derived from phytolith analyses (62). Because this node is likely to be significantly older than that (e.g., ref. 66), we also ran a second analysis assigning the same node an age of 65 Ma, as suggested by phytolith morphotypes from dinosaur coprolites (67). This second analysis did not change our inferences of the age of either Portulacineae or Cactaceae.

Dating analyses for the Cactaceae required a secondary calibration, where age estimates from the analysis of the 83-gene seed plant phylogeny were applied to a well-sampled phylogeny of Portulacineae and outgroups. Upper and lower constraints were set up for Portulacineae and Cactoideae (Fig. S2) by using the estimates obtained from the first two multidivtime analyses, where the oldest and youngest bounds of fossil ages were applied, respectively.

We used a likelihood-based method for identifying shifts in diversification rates by using the program MEDUSA (9), as implemented in R. MEDUSA allows users to "fill in" a phylogeny with all extant species by pruning the phylogeny down to the largest possible collection of monophyletic taxa where unsampled taxa may be confidently placed at one of the tips. This approach works well for groups with solid and detailed taxonomic classifications; unfortunately, higher-level taxonomy in the cacti is in a state of flux, and many of the currently recognized tribes and subtribes are known to be paraphyletic (2). Because of this uncertainty, if we were to include every species of Portulacineae in our MEDUSA run, we would be forced to reduce our 295-taxon tree to 42 tips; even worse, the core cacti would have only 5 tips. As an alternative, we used a genus level approach, given that genera circumscriptions have been recently revised and appear to be stabilizing (2, 68–70): We pruned our tree down to one exemplar per sampled genus and then added the total number of species in each genus to the tips (Fig. S3). We did not attempt to include genera that were not present in our 295-taxon tree. Many taxonomically problematic groups were lumped into single large genera to be conservative (e.g., *Echinopsis* includes *Chamaecereus*, *Helianthocereus*, *Lobivia*, *Pseudolobivia*, *Setiechinopsis*, *Soehrensia*, and *Trichocereus*). In the few cases where we had complete sampling for a genus (e.g., *Pereskia*, *Maihuenia*), we included all taxa. This approach enabled us to represent extant diversity quite well, with most major groups attaining >70% coverage and an average coverage across both Cactaceae and Portulacineae of 75% (Table S5). Outside of Portulacineae and Molluginaceae, our sampling was more limited. To ensure that this did not affect inferences inside Cactaceae, we ran MEDUSA only on a tree of Molluginaceae + Portulacineae (Fig. S3). Because of the uncertainty inherent in estimating speciation and extinction rates from phylogenetic topologies, we report MEDUSA rate estimates alongside a statistic assuming a simpler pure-birth model (i.e., assuming zero extinction): D ($D = [\ln(N_t) - \ln(N_o)]/T$ (Table 1 and Table S4), where T is the stem age of the clade, N_t is the number of taxa, and $N_o = 1$; ref. 71).

ACKNOWLEDGMENTS. We thank S. Albesiano, M. Alfaro, C. Blazier, J. Brown, F. Cáceres, A. Cano, D. Chatelet, C. Dunn, L. Garrison, F. Goetz, C. Hunkeler, D. Jarzen, R. Kiesling, S. Manchester, I. Peralta, A. Rahlin, D. Royer, S. Schmerler, S. Smith, D. Soltis, P. Soltis, V. Vincenzetti, and Z. Xi for assistance during plant collection and laboratory work, advice with analyses, and comments on the manuscript and the staff of various Herbarium/Botanical Gardens: BRU, FR, G, MERL, MO, NY, UPS, USM, Z, and ZSS (Table S2). This work was supported by National Science Foundation-Division of Environmental Biology Grant 1026611 (to E.J.E.).

1. Ogburn RM, Edwards EJ (2010) The ecological water-use strategies of succulent plants. *Adv Bot Res* 55:179–255.
2. Nyffeler R, Eggli U (2010) A farewell to dated ideas and concepts –molecular phylogenetics and a revised suprageneric classification of the family Cactaceae. Schumannia 6. *Biodiversity & Ecology* 3:109–149.
3. Gibson AC, Nobel PS (1986) *The Cactus Primer* (Harvard Univ Press, Cambridge, MA).
4. Axelrod DI (1979) Age and origin of Sonoran Desert vegetation. *Occ Pap Cal Acad Sci* 132:1–74.
5. Hershkovitz MA, Zimmer EA (1997) On the evolutionary origins of the cacti. *Taxon* 46: 217–232.
6. Nyffeler R (2002) Phylogenetic relationships in the cactus family (Cactaceae) based on evidence from trnK/matK and trnL-trnF sequences. *Am J Bot* 89:312–326.
7. Ocampo G, Columbus T (2010) Molecular phylogenetics of suborder Cactineae (Caryophyllales), including insights into photosynthetic diversification and historical biogeography. *Am J Bot* 97:1–21.
8. Moore MJ, Soltis PS, Bell CD, Burleigh JG, Soltis DE (2010) Phylogenetic analysis of 83 plastid genes further resolves the early diversification of eudicots. *Proc Natl Acad Sci USA* 107:4623–4628.
9. Alfaro ME, et al. (2009) Nine exceptional radiations plus high turnover explain species diversity in jawed vertebrates. *Proc Natl Acad Sci USA* 106:13410–13414.
10. Moore MJ, Bell CD, Soltis PS, Soltis DE (2007) Using plastid genome-scale data to resolve enigmatic relationships among basal angiosperms. *Proc Natl Acad Sci USA* 104:19363–19368.
11. Edwards EJ, Donoghue MJ (2006) *Pereskia* and the origin of the cactus life-form. *Am Nat* 167:777–793.
12. Nyffeler R, Eggli U, Ogburn M, Edwards E (2008) Variation on a theme: repeated evolution of succulent life forms in the Portulacineae (Caryophyllales). *Haseltonia* 14: 26–36.
13. Edwards EJ, Nyffeler R, Donoghue MJ (2005) Basal cactus phylogeny: implications of Pereskia (Cactaceae) paraphyly for the transition to the cactus life form. *Am J Bot* 92: 1177–1188.
14. Klak C, Reeves G, Hedderson T (2004) Unmatched tempo of evolution in Southern African semi-desert ice plants. *Nature* 427:63–65.
15. Good-Avila SV, Souza V, Gaut BS, Eguiarte LE (2006) Timing and rate of speciation in *Agave* (Agavaceae). *Proc Natl Acad Sci USA* 103:9124–9129.
16. Horn JW, et al. (2010) Are growth forms and photosynthetic pathways correlates of diversification in *Euphorbia* (Euphorbiaceae)? *Botany 2010,* p 91.
17. Moore MJ, Jansen RK (2006) Molecular evidence for the age, origin, and evolutionary history of the American desert plant genus *Tiquilia* (Boraginaceae). *Mol Phylogenet Evol* 39:668–687.
18. Catalano SA, Vilardi JC, Tosto C, Saidman BO (2008) Molecular phylogeny and diversification history of *Prosopis* (Fabaceae: Mimosoideae). *Biol J Linn Soc Lond* 93: 621–640.
19. Luebert F, Wen J (2008) Phylogenetic analysis and evolutionary diversification of Heliotropium sect. Cochranea (*Heliotropiaceae*) in the Atacama Desert. *Syst Bot* 33: 390–402.
20. Verboom GA, et al. (2009) Origin and diversification of the Greater Cape flora: ancient species repository, hot-bed of recent radiation, or both? *Mol Phylogenet Evol* 51:44–53.
21. Ferrusquía-Villafranca I, Gonzáles-Guzmán LI (2005) *Biodiversity, Ecosystems, and Conservation in Northern Mexico* (Oxford Univ Press, New York).
22. Gregory-Wodzicki KM (2010) Uplift history of the Central and Northern Andes: A review. *Geol Soc Am Bull* 112:1091–1105.
23. Cane MA, Molnar P (2001) Closing of the Indonesian seaway as a precursor to east African aridification around 3-4 million years ago. *Nature* 411:157–162.
24. Sepulchre P, et al. (2006) Tectonic uplift and Eastern Africa aridification. *Science* 313: 1419–1423.
25. Cerling TE, et al. (1997) Global vegetation change through the Miocene/Pliocene boundary. *Nature* 389:153–158.
26. Sage RF (2004) The evolution of C_4 photosynthesis. *New Phytol* 161:341–370.
27. Edwards EJ, et al. (2010) C4 Grasses Consortium (2010) The origins of C_4 grasslands: Integrating evolutionary and ecosystem science. *Science* 328:587–591.

28. Christin P-A, Osborne CP, Sage RF, Arakaki M, Edwards EJ (2011) C4 eudicots are not younger than C4 monocots. *J Exp Bot*, 10.1093/jxb/err041.
29. Zachos J, Pagani M, Sloan L, Thomas E, Billups K (2001) Trends, rhythms, and aberrations in global climate 65 Ma to present. *Science* 292:686–693.
30. Ruddiman WF (2010) A paleoclimatic enigma? *Science* 328:838–839.
31. Huang Y, et al. (2007) Large scale hydrological change drove the late Miocene C_4 plant expansion in the Himalayan foreland and Arabian Peninsula. *Geology* 35: 531–534.
32. Dettman DL, et al. (2001) Seasonal stable isotope evidence for a strong Asian monsoon throughout the past 10.7 m.y. *Geol Soc Am* 1:31–34.
33. Tripati AK, Roberts CD, Eagle RA (2009) Coupling of CO2 and ice sheet stability over major climate transitions of the last 20 million years. *Science* 326:1394–1397.
34. Ehleringer JR, Monson RK (1993) Evolutionary and ecological aspects of photosynthetic pathway variation. *Annu Rev Ecol Syst* 24:411–439.
35. Jansen RK, et al. (2005) Methods for obtaining and analyzing whole chloroplast genome sequences. *Methods Enzymol* 395:348–384.
36. Chevreux B (1997–2010) MIRA V1-V3. Dept. of Molecular Biophysics, Deutsches Krebsforschungszentrum Heidelberg, Germany. Available at http://sourceforge.net/apps/mediawiki/mira-assembler. Accessed November 9, 2009.
37. Wyman SK, Jansen RK, Boore JL (2004) Automatic annotation of organellar genomes with DOGMA. *Bioinformatics* 20:3252–3255.
38. O'Quinn RL, Hufford L (2005) Molecular systematics of Montieae (Portulacaceae): Implications for taxonomy, biogeography and ecology. *Syst Bot* 30:314–331.
39. Mathews S, Lavin M, Sharrock RA (2005) Evolution of the phytochrome gene family and its utility for phylogenetic analyses of Angiosperms. *Ann Mo Bot Gard* 82: 296–321.
40. Christin P-A, et al. (2011) Complex evolutionary transitions and the significance of c_3-c_4 intermediate forms of photosynthesis in Molluginaceae. *Evolution* 65:643–660.
41. Edgar RC (2004) MUSCLE: A multiple sequence alignment method with reduced time and space complexity. *BMC Bioinformatics* 5:113.
42. Stamatakis A (2006) RAxML-VI-HPC: maximum likelihood-based phylogenetic analyses with thousands of taxa and mixed models. *Bioinformatics* 22:2688–2690.
43. Rutschmann F (2006) Molecular dating of phylogenetic trees: A brief review of current methods that estimate divergence times. *Divers Distrib* 12:35–48.
44. Yang Z (1993) Maximum-likelihood estimation of phylogeny from DNA sequences when substitution rates differ over sites. *Mol Biol Evol* 10:1396–1401.
45. Thorne JL, Kishino H, Painter IS (1998) Estimating the rate of evolution of the rate of molecular evolution. *Mol Biol Evol* 15:1647–1657.
46. Thorne JL, Kishino H (2002) Divergence time and evolutionary rate estimation with multilocus data. *Syst Biol* 51:689–702.
47. Mapes G, Rothwell GW (1984) Permineralized ovulate cones of Lebachia from Late Paleozoic Hamilton Quarry area in southeastern Kansas. *Palaeontology* 27:69–94.
48. Hughes NF (1994) *The Enigma of Angiosperm Origins* (Cambridge Univ Press, Cambridge, UK).
49. Friis EM, Eklund H, Pedersen KR, Crane PR (1994) Virginianthus calycanthoides gen. et sp. nov. – a calycanthaceous flower from the Potomac Group (early Cretaceous) of eastern North America. *Int J Plant Sci* 155:772–785.
50. Crepet WL, Nixon KC, Gandolfo MA (2004) Fossil evidence and phylogeny: The age of major angiosperm clades based on mesofossil and macrofossil evidence from Cretaceous deposits. *Am J Bot* 91:1666–1682.
51. Crane PR, Pedersen KR, Friis EM, Drinnan AN (1993) Early Cretaceous (early to middle Albian) platanoid inflorescences associated with sapindopsis leaves from the Potomac Group of eastern North America. *Syst Bot* 18:328–344.
52. Pedersen KR, Friis EM, Drinnan AN (1994) Reproductive structures of an extinct platanoid from the early Cretaceous (latest Albian) of eastern North America. *Rev Palaeobot Palynol* 80:291–303.
53. Friis EM, Crane PR, Pedersen KR (1988) The reproductive structures of Cretaceous Platanaceae. *Biologiske Skrifter* 31:1–55.
54. Manchester SR, O'Leary EL (2010) Phylogenetic distribution and identification of fin-winged fruits. *Bot Rev* 76:1–82.
55. Crepet WL, Nixon KC (1998) Fossil Clusiaceae from the Late Cretaceous (Turonian) of New Jersey and implications regarding the history of bee pollination. *Am J Bot* 85: 1122–1133.
56. Sims HJ, Herendeen PS, Lupia R, Christopher RA, Crane PR (1999) Fossil flowers with Normapolles pollen from the Upper Cretaceous of southeastern North America. *Rev Palaeobot Palynol* 106:131–151.
57. Knobloch E, Mai DH (1986) Monographie der Früchte und Samen in der Kreide von Mitteleuropa. *Rozpravy ústredního ústavu geologickénho Praha* 47:1–219.
58. Nichols DJ, Traverse A (1971) Palynology, petrology, and depositional environments of some early Tertiary lignites in Texas. *Geosci & Man* 3:37–48.
59. Collinson ME, Boulter MC, Holmes PL (1993) *The Fossil Record 2* (Chapman & Hall, London).
60. Call BV, Dilcher DL (1992) Investigations of angiosperms from the Eocene of southwestern North America: Samaras of *Fraxinus wilcoxiana* Berry. *Rev Palaeobot Palynol* 74:249–266.
61. Barreda VD, et al. (2010) Eocene Patagonia fossils of the daisy family. *Science* 329: 1621.
62. Strömberg CAE (2005) Decoupled taxonomic radiation and ecological expansion of open-habitat grasses in the Cenozoic of North America. *Proc Natl Acad Sci USA* 102: 11980–11984.
63. Cevallos-Ferriz SRS, Estrada-Ruiz E, Pérez-Hernández BR (2008) Phytolaccaceae infrutescence from Cerro del Pueblo Formation, Upper Cretaceous (Late Campanian), Coahuila, Mexico. *Am J Bot* 95:77–83.
64. Crepet WL, Feldman GD (1991) The earliest remains of grasses in the fossil record. *Am J Bot* 78:1010–1014.
65. Linder HP (1986) The evolutionary history of the Poales/Restionales – a hypothesis. *Kew Bull* 42:297–318.
66. Christin P-A, et al. (2008) Oligocene CO_2 decline promoted C_4 photosynthesis in grasses. *Curr Biol* 18:37–43.
67. Prasad V, Strömberg CAE, Alimohammadian H, Sahni A (2005) Dinosaur coprolites and the early evolution of grasses and grazers. *Science* 310:1177–1180.
68. Anderson EF (2001) *The Cactus Family* (Timber, Portland, OR).
69. Hunt DH, et al. (2006) *The New Cactus Lexicon* (DH Books, Milborne Port, Sherborne, England).
70. Nyffeler R, Eggli U (2010) Disintegrating Portulacaceae: A new familial classification of the suborder Portulacineae (Caryophyllales) based on molecular and morphological data. *Taxon* 1:227–240.
71. Baldwin BG, Sanderson MJ (1998) Age and rate of diversification of the Hawaiian silversword alliance (Compositae). *Proc Natl Acad Sci USA* 95:9402–9406.

Supporting Information

Arakaki et al. 10.1073/pnas.1100628108

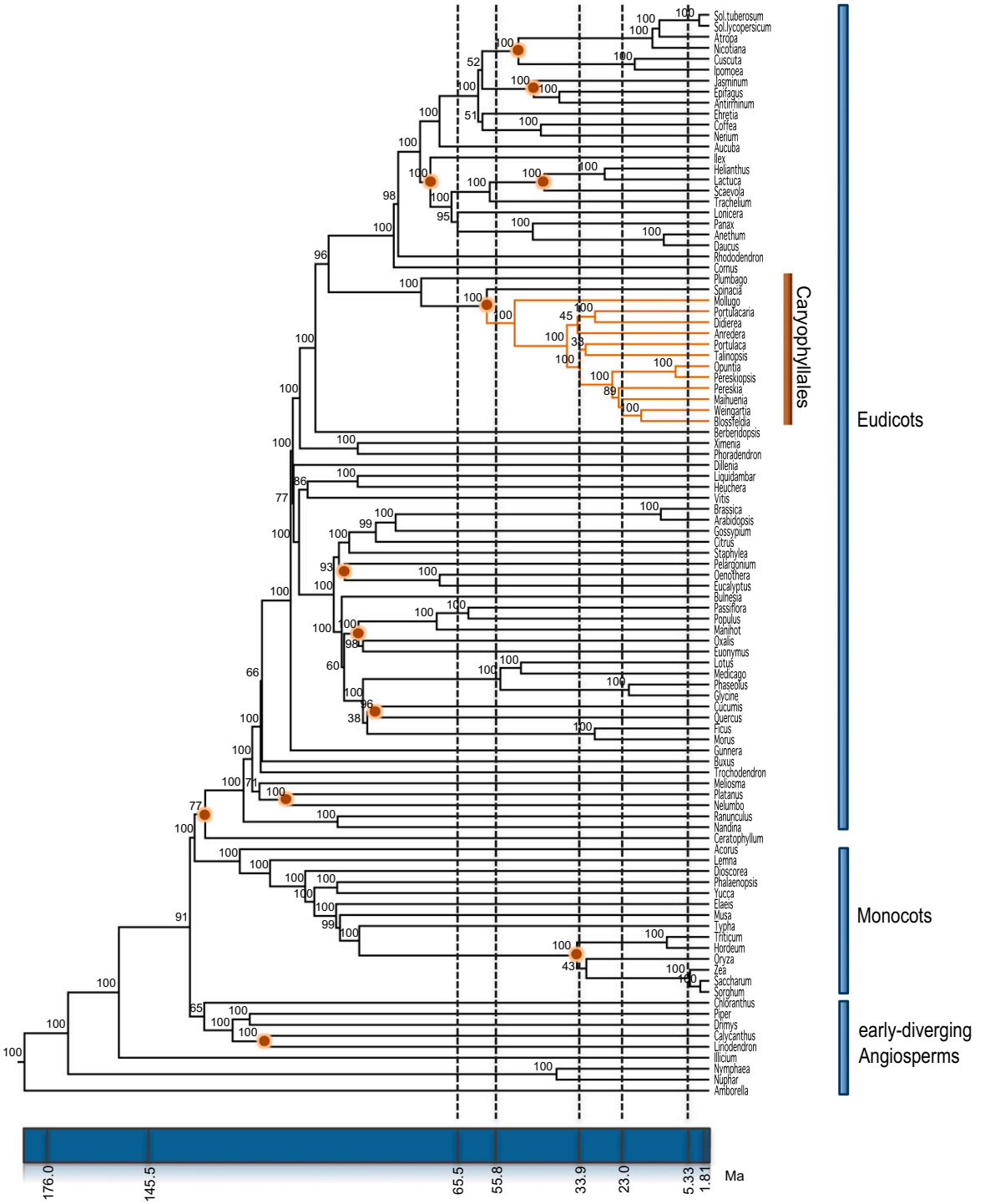

Fig. S1. Chronogram of Angiosperms. Divergence times were estimated with Multidivtime on a ML tree of 102 taxa and 83 chloroplast genes. Clade in orange includes additions to analysis by Moore et al. (1) to increase sampling in the Caryophyllales. Dots indicate placement of fossil constraints applied to dating analyses. Bootstrap values are above the branches. The root is not shown.

1. Moore MJ, Soltis PS, Bell CD, Burleigh JG, Soltis DE (2010) Phylogenetic analysis of 83 plastid genes further resolves the early diversification of eudicots. *Proc Natl Acad Sci USA* 107:4623–4628.

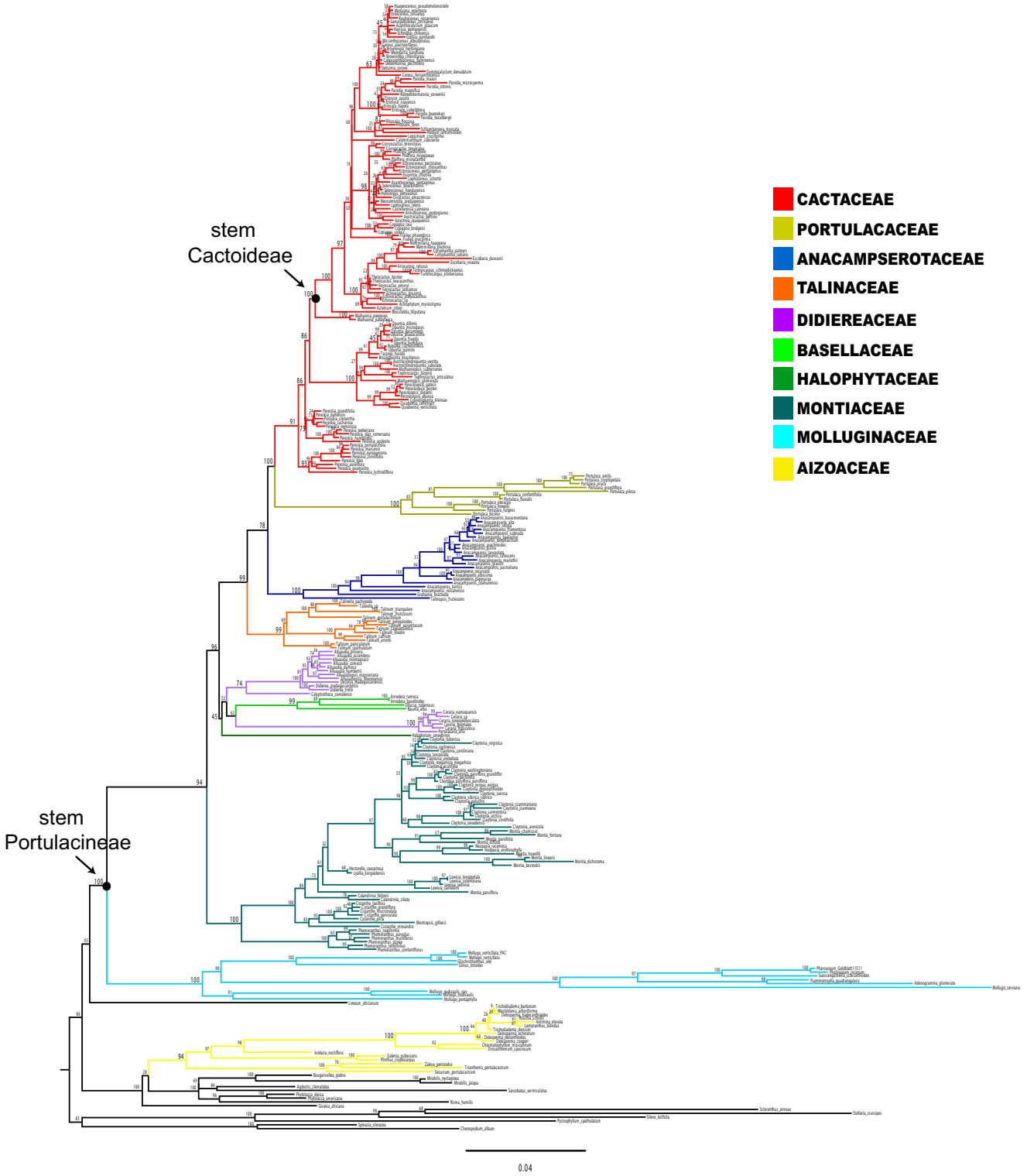

Fig. S2. Maximum likelihood phylogram based on sequences of nuclear *PHYC* and chloroplast *trnK/matK* genes for 295 taxa representing the Portulacineae and outgroups. Black dots indicate placement of age constraints in secondary dating analyses. Numbers above the branches are likelihood bootstrap support values.

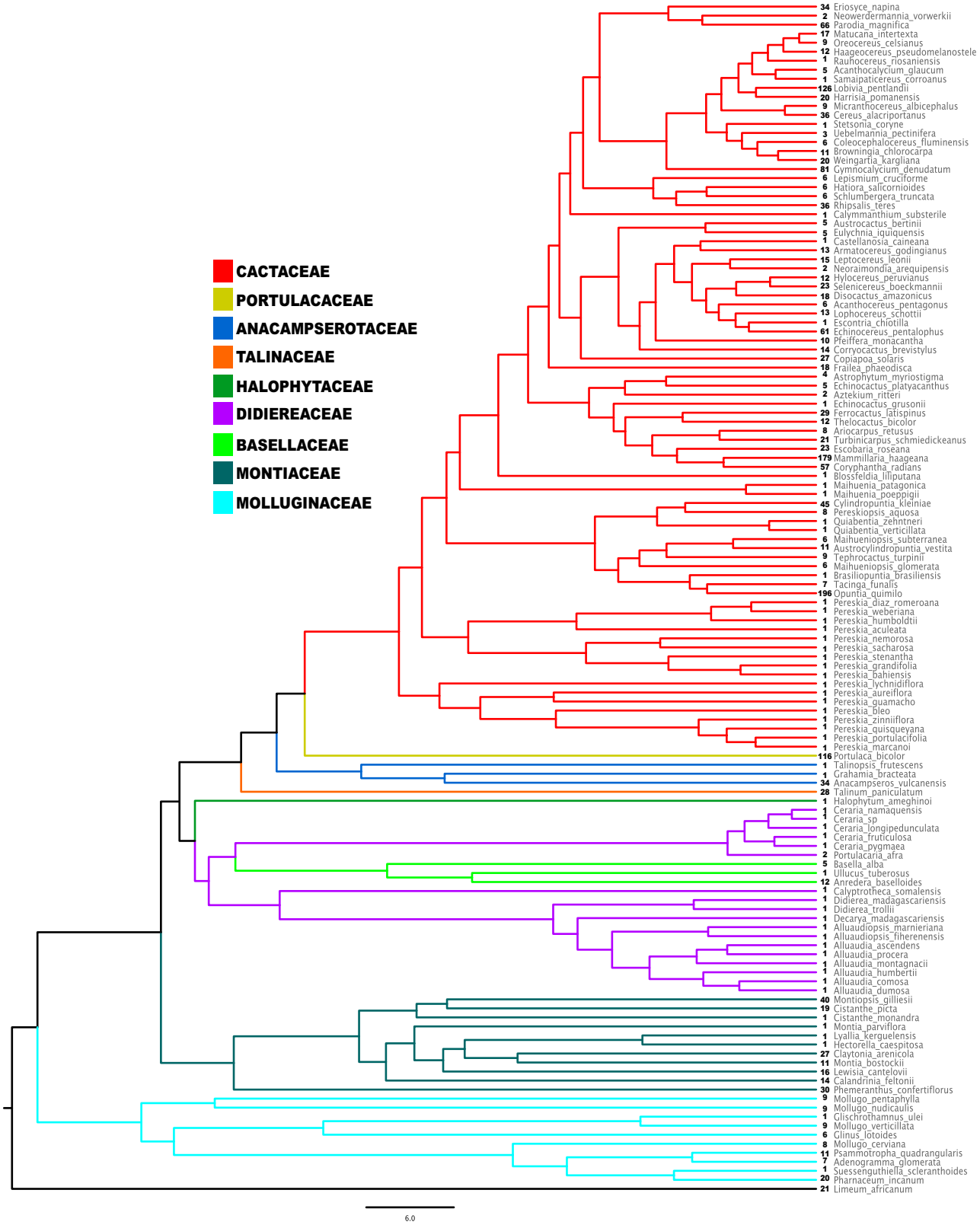

Fig. S3. Calibrated tree from Fig. 1, pruned to representative taxa for MEDUSA analyses. The number of species that each taxon in the tree represents is placed alongside tip names. Outgroups were excluded from MEDUSA analyses because of lower representation of taxa.

Other Supporting Information Files

Table S1 (DOC)
Table S2 (DOC)
Table S3 (DOC)
Table S4 (DOC)
Table S5 (DOC)